

# ***In situ* synthesis and encapsulation of copper phthalocyanine into MIL-101(Cr) and MIL-100(Fe) pores and investigation of their catalytic performance in the epoxidation of styrene**

**Ardeshir Dadgar Yeganeh, Mostafa M. Amini\* and Nasser Safari<sup>‡</sup>**

*Department of Chemistry, Shahid Beheshti University, G.C., Tehran 1983963113, Iran.*

*Received 7 July 2019*

*Accepted 5 September 2019*

**ABSTRACT:** In this work, copper phthalocyanine (CuPc) was encapsulated into mesocages of MIL-101(Cr) and MIL-100(Fe) by assembling CuPc's constitutional fractions using a deep eutectic solvent. The prepared materials, CuPc@MIL-101(Cr) and CuPc@MIL-100(Fe), were characterized by powder X-ray diffraction (PXRD), FT-IR, UV-vis and diffuse reflectance UV (DR-UV) spectroscopies, scanning electron microscopy (SEM), transmission electron microscopy (TEM), and ICP-OES spectrometry. The prepared materials were used as heterogeneous catalysts for catalytic epoxidation of styrene with molecular oxygen and also *tert*-butyl hydroperoxide (TBHP) as oxidants in acetonitrile as a solvent. The impact of MOFs and the role of the CuPc complex as the active species in the MOFs' cages in the epoxidation of styrene were investigated. Among the prepared catalysts, CuPc@MIL-101(Cr) showed the best performance. The heterogeneity of the catalysts was examined by a hot filtration test and ICP-OES of the filtrates after the reaction. Spent catalysts were analyzed by PXRD, FT-IR, UV-DRS, and TEM for reusability investigation and also to further explore the heterogeneous nature of the hybrid materials. Results showed that the prepared catalysts could be recycled and used for several consecutive times without a considerable drop in activity.

**KEYWORDS:** MIL-101(Cr); MIL-100(Fe); metallophthalocyanine; epoxidation.

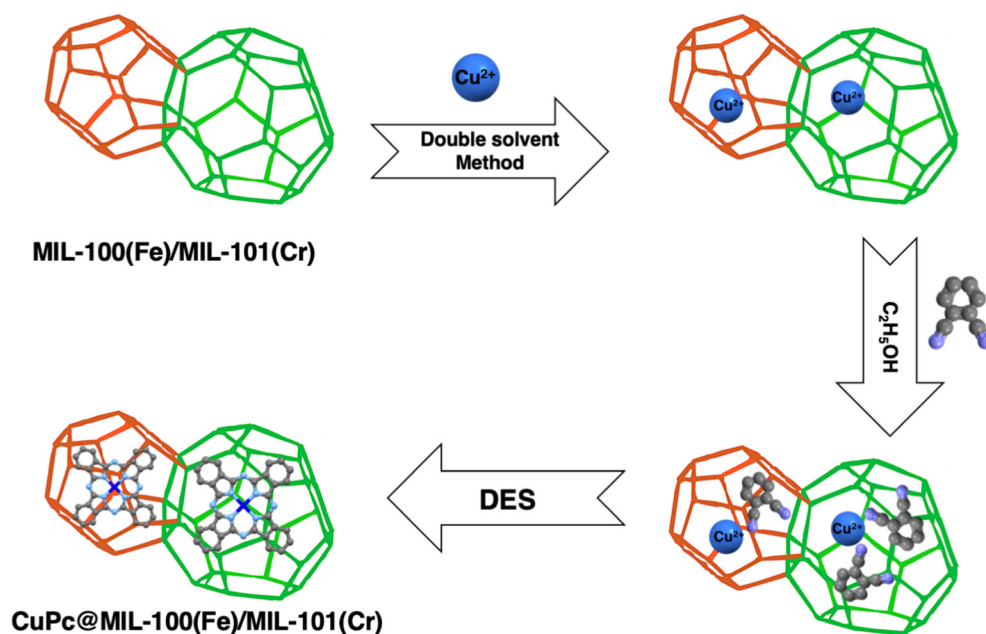
## **INTRODUCTION**

The selective epoxidation of styrene has attracted notable attention in view of the fact that the epoxy product is an essential intermediate in the synthesis of pharmaceuticals and fine chemicals [1, 2]. Conventionally, stoichiometric amounts of peracids like PhIO have been used to perform epoxidation reactions, but major disadvantages such as high cost, difficulty of handling, lack of selectivity toward epoxy and formation of unwanted wastes have led to serious environmental and economic concerns [3, 4]. Thus, the epoxidation of styrene by employing more benign and environmentally friendly oxidants like molecular oxygen has been found to be a promising alternative to the traditional route [5–7].

The use of Metal-Organic Frameworks (MOFs) in the field of heterogeneous catalysis has grown exponentially over the last decade [8, 9]. Despite high concentrations of metal centers with coordinately unsaturated or exchangeable positions which can perform as catalytic active sites, remarkable features such as high porosity with regular pores and large surface areas, framework flexibility, low framework density and large empty space, have made MOFs promising candidates as solid matrices for immobilization of transition metal complexes and nanoparticles [10–14]. Among porous materials, MIL-100 and MIL-101 MOFs are two examples of large non-proteinic structures which have been designed so far and used extensively both as catalysts and supports in liquid-phase reactions such as catalytic oxidation [15–22]. These MOFs circumvent some of the major drawbacks of their counterparts in heterogeneous catalyzes, such as thermal [23] and chemical [24] instability and lack of resistance toward active site leaching under reaction conditions [25].

<sup>‡</sup> SPP full member in good standing.

\*Correspondence to: Mostafa M. Amini, tel.: +98-21-29903109, fax: +9-21-22431663, email: m-pouramini@sbu.ac.ir.



**Scheme 1.** Schematic representation of CuPc synthesis within the pores of MIL-101(Cr) or MIL-100(Fe)

Immobilization of polyoxometalates into MIL-100(Fe) and MIL-101(Cr) has provided highly efficient and stable heterogeneous catalysts for epoxidation of alkenes and benzyl alcohol oxidation, respectively [26, 27]. Other metal complexes and metal nanoparticles have also been incorporated within the cages of the earlier mentioned MOFs in order to catalyze various organic transformations [28–32].

The activity of coordination complexes as homogeneous catalysts is well established [33–35], but from an industrial point of view, the heterogenization of homogeneous catalysts by immobilizing them into appropriate solid support provides easy recovery and reusability as two significant advantages of this approach [36, 37]. In this context, phthalocyanine metal complexes (MPcs), which are a substantial class of coordination compounds, have become the center of attention in past decades due to their facile large-scale preparation and chemical and thermal stability. These factors make MPcs great candidates as catalysts, especially in oxidation reactions [38]. Different strategies, including electrostatic interaction [39], covalent anchoring [40], impregnation, and encapsulation inside porous structures have been applied for immobilization of MPcs in supports. The impregnation approach is limited because of MPcs' low solubility in common organic solvents; this consequently necessitates the usage of substituted MPcs which are soluble but challenging to synthesize such as FePcS and RuPcF<sub>16</sub> that are encapsulated inside MIL-101(Cr) *via* this method and used in oxidation reactions [41, 42]. In 2014, Ma and coworkers introduced a new strategy to encapsulate CoPc into the pores of bio-MOF [43], but a requirement to use anionic MOF and a long reaction

process alongside a grueling work-up has limited this method. The catalytic activity of the constructed material by a new strategy was examined in the epoxidation of styrene with TBHP as the oxidant, and 72% conversion with 65% selectivity to styrene oxide was obtained. Recently, Boroujeni *et al.* reported a straightforward and green procedure to encapsulate MPcs by loading their constituents inside the internal voids of MIL-101 and then employing an ionic liquid to synthesize the desired MPc@MIL-101 [44].

Herein, we further investigate the potential of the reported strategy for encapsulating copper phthalocyanine (CuPc) inside the pores of MIL-100(Fe) as well as MIL-101(Cr) using deep eutectic solvent (DES) which recently has been reported by Shaabani *et al.* [45] to synthesize MPc complexes in a shorter reaction time and at a lower temperature than conventional routes. The obtained materials have been characterized by PXRD, FT-IR, UV-Vis, UV-DRS, SEM, TEM and N<sub>2</sub> adsorption-desorption techniques. The catalytic performance and heterogeneity of the prepared catalysts in the styrene epoxidation with O<sub>2</sub> and aqueous TBHP have also been studied. Scheme 1 illustrates *in situ* synthesis and encapsulation of copper phthalocyanine into MIL-101(Cr) and MIL-100(Fe).

## RESULTS AND DISCUSSION

### Characterization of precursors and catalysts

The synthesis of MIL-101(Cr) and MIL-100(Fe) was confirmed by powder X-ray diffraction (PXRD) analysis (Figs 1 and 2). The diffraction patterns are well matched

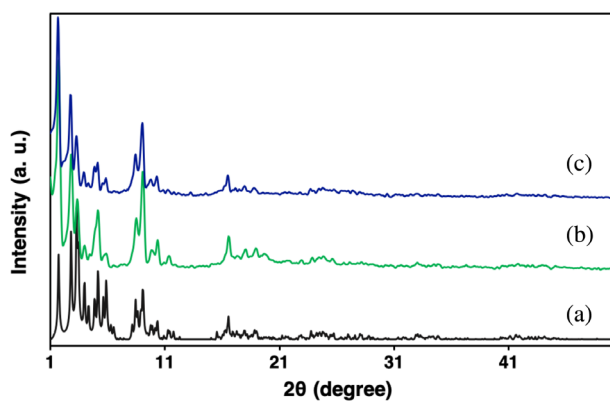


Fig. 1. PXRD patterns of (a) Simulated MIL-101(Cr), (b) As-synthesized MIL-101(Cr) and (c) CuPc@MIL-101(Cr)

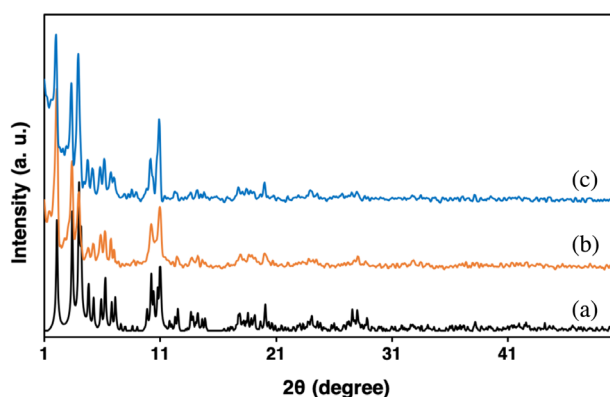


Fig. 2. PXRD patterns of (a) Simulated MIL-100(Fe), (b) As-synthesized MIL-100(Fe) and (c) CuPc@MIL-100(Fe)

to the simulated ones which were obtained from their crystallographic information files (CIFs). As is shown, the synthesis of CuPc inside the pores of MIL-100(Fe) and MIL-101(Cr) did not affect the reflections of these MOFs, indicating that their structural integrities are maintained. Since the characteristic reflections of free CuPc complex according to ICDD card no. 11-0893 were not detected in diffractograms, it can be assumed that the CuPc is highly dispersed inside the pores of the MOFs [44].

The FT-IR spectrum of MIL-101(Cr) (Fig. 3a) reveals characteristic vibrational bands of the framework O–C–O at 1398 and 1612  $\text{cm}^{-1}$ , which corresponds to the asymmetric and symmetric stretching modes, respectively [46]. Also, a benzene ring C=C, stretching vibration at 1508  $\text{cm}^{-1}$ , and C–H deformation vibrations at 1157, 1018, and 748  $\text{cm}^{-1}$  are observed in the spectrum [47]. Typical characteristic bands of MIL-100(Fe) (Fig. 4a) at 1627, 1450, and 1370  $\text{cm}^{-1}$  are allocated to C=O stretching vibration and asymmetrical and symmetrical vibrations of O–C–O carboxylate group, respectively [48]. Moreover, the bands at 760 and 710  $\text{cm}^{-1}$  in the fingerprint region are assigned to C–H bending vibrations

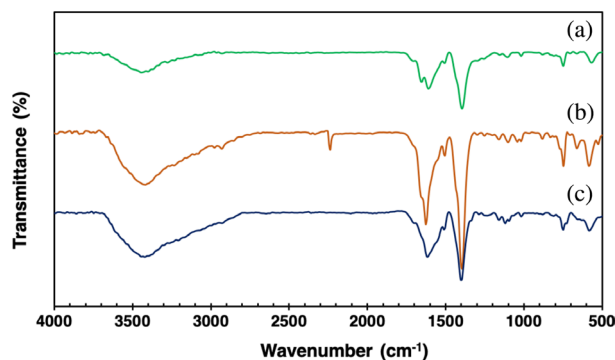


Fig. 3. FT-IR spectra of (a) MIL-101(Cr), (b)  $\text{Cu}^{2+}$ -phthalonitrile@MIL-101(Cr) and (c) CuPc@MIL-101(Cr)

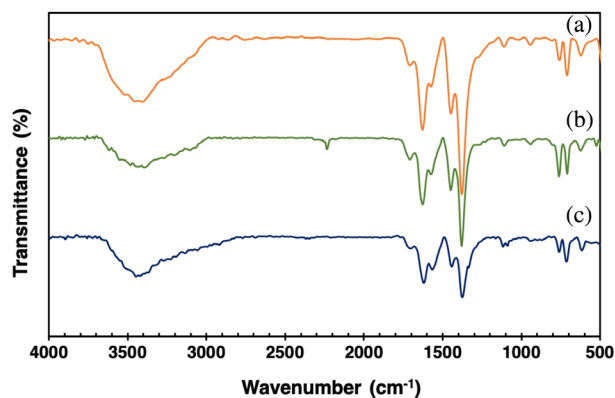


Fig. 4. FT-IR spectra of (a) MIL-100(Fe), (b)  $\text{Cu}^{2+}$ -phthalonitrile@MIL-100(Fe) and (c) CuPc@MIL-100(Fe)

of the aromatic ring [49]. After loading of phthalonitrile into  $\text{Cu}^{2+}$ @MIL-100(Fe) and MIL-101(Cr), a band around 2230  $\text{cm}^{-1}$  appears in their spectrum which is ascribed to CN stretching vibration (Figs 3b and 4b), but after the cyclotetramerization of phthalonitrile this band disappeared, which can corroborate the successful synthesis of CuPc inside the MOFs [44, 50]. Other weak bands at 1087, 1118, and a shoulder near 1334  $\text{cm}^{-1}$ , which are the characteristic vibrations of CuPc, can be seen in the FT-IR spectrum of CuPc@MIL-101(Cr) and CuPc@MIL-100(Fe) (Figs 3c and 4c) [51].

To investigate the encapsulation of CuPc within the pores of MIL-101(Cr), and MIL-100(Fe), CuPc was extracted from MIL-101(Cr) and MIL-100(Fe) and their UV-vis was recorded. As Fig. 5 shows, the spectra demonstrate two absorption bands at 702 and 795 nm, arising from  $\pi \rightarrow \pi^*$  charge transfer from  $a_{1g}$  to  $e_g$  orbitals, known as Q bands [52, 53]. Those bands are the characteristic bands of CuPc in concentrated sulfuric acid. They appeared after extraction of CuPc from the MOFs and are ascribed to planar  $D_{4h}$  symmetry in solutions [54]. Moreover, an absorption band became visible at around 440 nm, known as the Soret or B band, and is attributed to another ligand centered  $\pi \rightarrow \pi^*$  transition from  $a_{2u}$  to  $e_g$

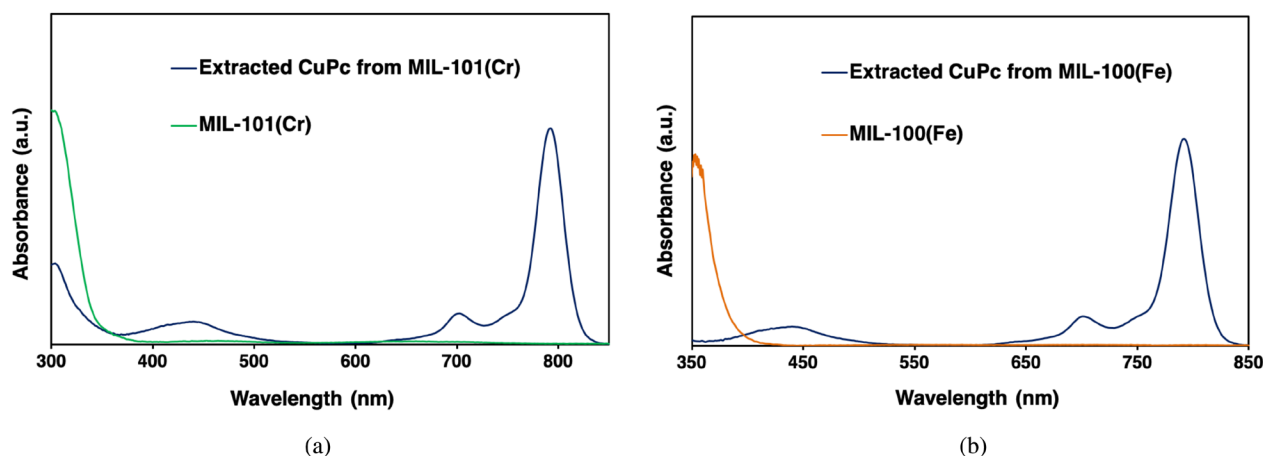


Fig. 5. UV-vis spectra of (a) Extracted CuPc from MIL-101(Cr), (b) Extracted CuPc from MIL-100(Fe)

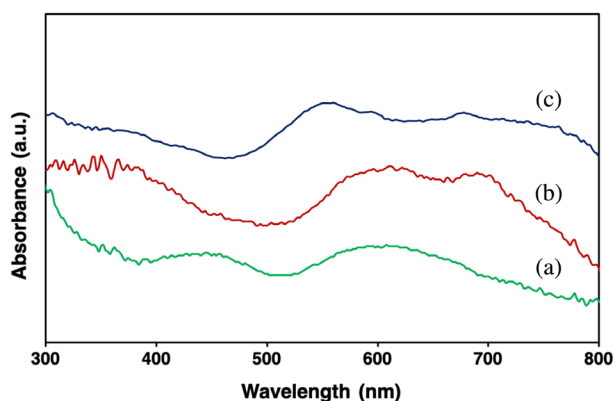


Fig. 6. UV-DR spectrum of (a) MIL-101(Cr), (b) CuPc@MIL-101(Cr) and (c) Neat CuPc complex

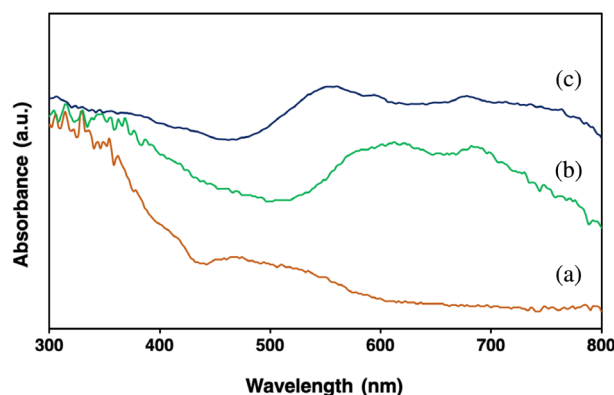


Fig. 7. UV-DR spectrum of (a) MIL-100(Fe), (b) CuPc@MIL-100(Fe) and (c) Neat CuPc complex

orbitals [52–54]. Therefore, it can be concluded that the CuPc remained intact after encapsulation in the MOFs.

The presence of CuPc inside the MOFs is also confirmed by diffuse reflectance UV-vis spectroscopy, as shown in Figs 6 and 7. Neat CuPc complex displayed broadened and resolved bands in the 550–750 nm region, indicating a non-planar geometry for the complex. After accommodation of CuPc inside the pores of MIL-100(Fe) and MIL-101(Cr), those bands shifted to around 680 and 610 nm and can be assigned to Q(0,0) and Q(0,1) transitions of monomeric and dimeric species, respectively. The red shift and reduction of split bands after the encapsulation of CuPc inside the MOFs suggests that the CuPc molecules are highly dispersed and within the MOFs cavities [54–56].

SEM images were taken to investigate the morphology and structure of the MOFs before and after the encapsulation of CuPc complexes. As revealed in Fig. 8, the structures of MIL-100(Fe) and MIL-101(Cr) remained intact after encapsulation of CuPc molecules inside their pores, confirming that the preparation process does not affect the MOFs' structures. Furthermore, particle

sizes of MIL-101(Cr) (300–600 nm) and MIL-100(Fe) (200–500 nm) were unaltered after incorporation of CuPc molecules, although a low extent of agglomeration of particles was observed in the case of CuPc@MIL-100(Fe) (Fig. 8d). TEM images further confirm that the shape and size of the MOF particles were retained after the encapsulation of CuPc complexes inside their structures (Figs 8e and 8f).

The N<sub>2</sub> adsorption–desorption isotherms of bare and CuPc-encapsulated MOFs are given in Figs 9 and 10. Both MIL-101(Cr) and CuPc@MIL-101(Cr) revealed type I(b) isotherms with H4 hysteresis loops, which are exhibited in the presence of micropores and narrow mesopores, according to IUPAC classification [57]. MIL-100(Fe) and CuPc@MIL-100(Fe) also displayed H4 hysteresis loops with mixed type I/IV isotherms, and they related to materials with microporous windows and mesoporous cages [58]. The textural parameters of the prepared materials are shown in Table 1. The BET-specific surface area and pore volume of MIL-101(Cr) are 2437 m<sup>2</sup> g<sup>−1</sup> and 1.15 cm<sup>3</sup> g<sup>−1</sup>, and for MIL-100(Fe) are 1248 m<sup>2</sup> g<sup>−1</sup> and 0.72 cm<sup>3</sup> g<sup>−1</sup>, respectively. These values



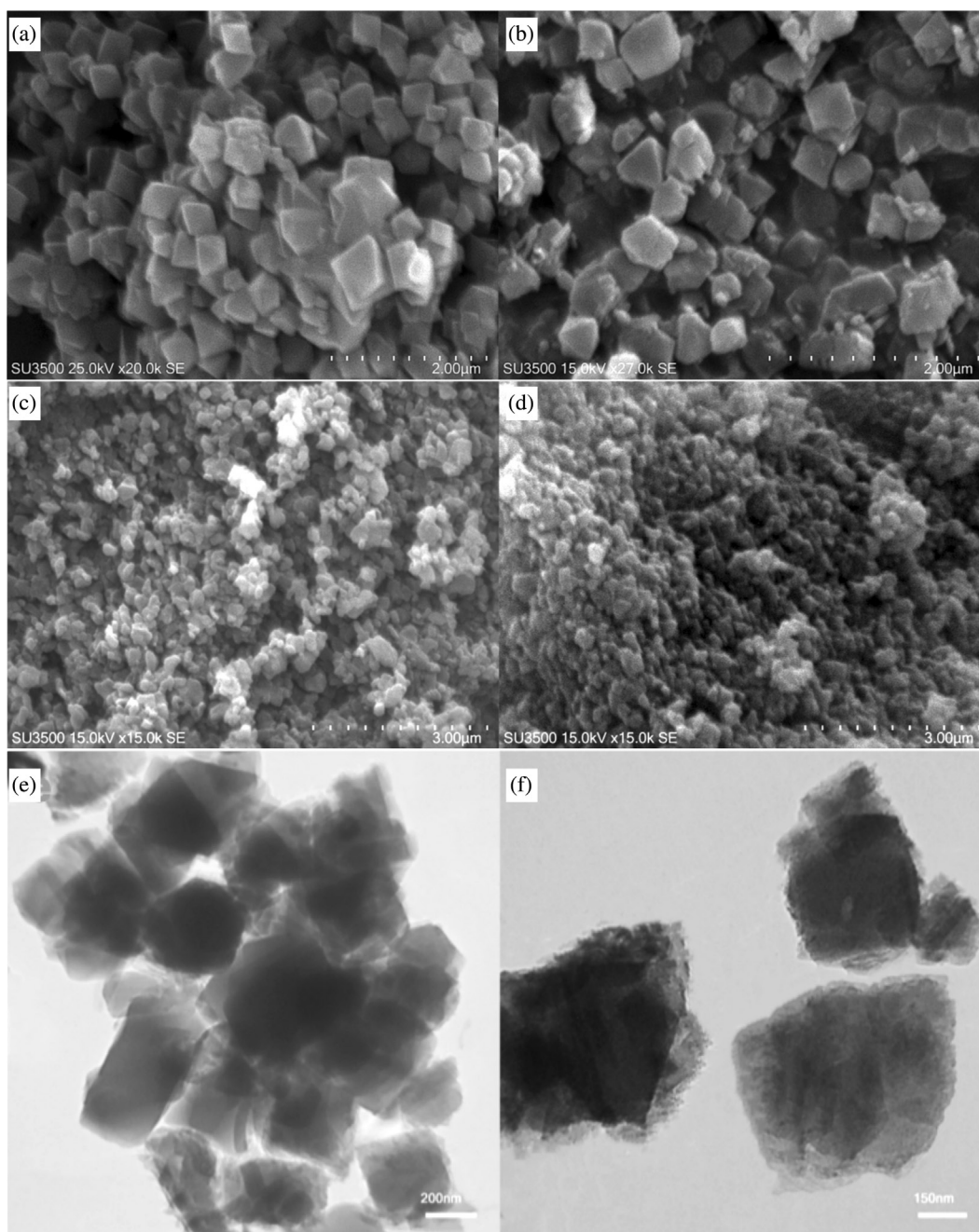


**Fig. 8.** SEM images of (a) MIL-101(Cr), (b) CuPc@MIL-101(Cr), (c) MIL-100(Fe) and (d) CuPc@MIL-100(Fe). TEM images of (e) CuPc@MIL-101(Cr) and (f) CuPc@MIL-100(Fe)

decreased to  $2262 \text{ m}^2 \text{ g}^{-1}$  and  $0.91 \text{ cm}^3 \text{ g}^{-1}$  after incorporation of CuPc in MIL-101(Cr), and to  $1104 \text{ m}^2 \text{ g}^{-1}$  and  $0.55 \text{ cm}^3 \text{ g}^{-1}$  after inclusion in MIL-100(Fe), respectively. The decrease of specific surface areas and pore volumes of the encapsulated samples indicates the presence of CuPc complexes within the cavities of the MOFs. The amount of CuPc in the pores of MIL-100(Fe) and MIL-101(Cr) was obtained by ICP-OES, and a value of 10.1 and 17.5 wt.% loading was acquired for CuPc@MIL-100(Fe) and CuPc@MIL-101(Cr), respectively (Table 1).

### Catalytic studies

The catalytic activity of the prepared solids was investigated in the epoxidation of styrene in two optimized reaction conditions: one with  $\text{O}_2$  as oxidant and *iso*-butyraldehyde as co-reductant (Table 2), and the other with aqueous TBHP as oxidant (Table 3) in acetonitrile media. At first, the reaction in the absence of catalyst was performed in both systems, and low conversions of styrene were observed (Tables 2 and 3, entry 1). These results indicate the importance of catalysts' role in the

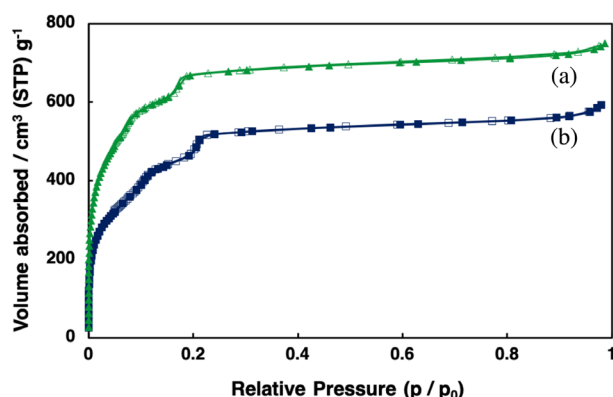


**Fig. 9.** N<sub>2</sub> adsorption-desorption isotherms of (a) MIL-101(Cr) and (b) CuPc@MIL-101(Cr)

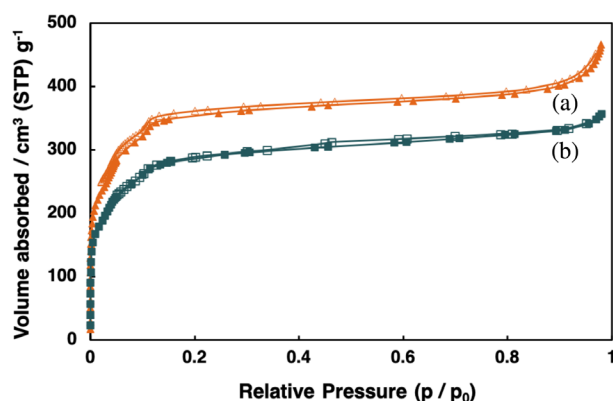


**Fig. 10.** N<sub>2</sub> adsorption-desorption isotherms of (a) MIL-100(Fe) and (b) CuPc@MIL-100(Fe)

reaction progression. The reaction with activated MIL-101(Cr) in the O<sub>2</sub>/*iso*-butyraldehyde system resulted in 53.4% styrene conversion with 72.4% selectivity towards styrene oxide (Table 2, entry 3). Moreover, MIL-100(Fe)

demonstrated activity in the epoxidation of styrene with 49.8% conversion and 55.3% selectivity to the epoxy product with molecular oxygen as oxidant (Table 2, entry 4). The catalytic activity of the MOFs was also

**Table 1.** Textural properties and the amount of CuPc in the samples

Samples	S <sub>BET</sub> (m <sup>2</sup> g <sup>-1</sup> )	V <sub>Total</sub> (cm <sup>3</sup> g <sup>-1</sup> ) <sup>a</sup>	CuPc content (wt.%) <sup>b</sup>
MIL-101(Cr)	2437	1.15	—
CuPc@MIL-101(Cr)	2262	0.91	17.58
MIL-100(Fe)	1248	0.72	—
CuPc@MIL-100(Fe)	1104	0.55	10.1

<sup>a</sup>V<sub>Total</sub> was measured at P/P<sub>0</sub> = 0.98. <sup>b</sup>Determined by ICP-OES.

**Table 2.** catalyst screening in the epoxidation of styrene using O<sub>2</sub> as oxidant<sup>a</sup>

Entry	Catalyst	Conversion (%)	Selectivity (%)		
			SO	B	OP <sup>b</sup>
1	No catalyst	10.6	47.2	33.2	19.6
2 <sup>c</sup>	CuPc	52.5	63.6	23.1	13.3
3 <sup>d</sup>	MIL-101(Cr)	53.4	72.4	19.2	13.4
4 <sup>d</sup>	MIL-100(Fe)	49.8	55.3	27.6	17.1
5	CuPc@MIL-101(Cr)	100	85	9.1	5.9
6	CuPc@MIL-100(Fe)	82.8	76.8	10.3	12.9
7 <sup>e</sup>	CuPc@MIL-101(Cr)	100	80.6	10	9.4
8 <sup>f</sup>	CuPc@MIL-100(Fe)	80.1	75.2	8.1	16.7

<sup>a</sup>Reaction conditions: styrene (1 mmol), catalyst (0.15 mol% based on Cu), CH<sub>3</sub>CN (2 ml), O<sub>2</sub> balloon (1 atm), *iso*-butyraldehyde (3 mmol), temperature (60 °C), time (4 h). <sup>b</sup>Other products including phenylacetaldehyde and benzoic acid. <sup>c</sup>0.8 mg CuPc was used. <sup>d</sup>5 mg MOF was used. <sup>e</sup>4th run. <sup>f</sup>3rd run.

**Table 3.** catalyst screening in the styrene epoxidation using TBHP as oxidant<sup>a</sup>

Styrene  $\xrightarrow[\text{TBHP, 80 } ^\circ\text{C, 7h}]{\text{Catalyst, CH}_3\text{CN}}$  Styrene Oxide (SO) + Benzaldehyde (B) + Other Products (OP)

Entry	Catalyst	Conversion (%)	Selectivity (%)		
			SO	B	OP <sup>b</sup>
1	No catalyst	17.1	35.3	46.3	18.5
2 <sup>c</sup>	CuPc	66.8	61.3	32.4	6.3
3 <sup>d</sup>	MIL-101(Cr)	45.9	38.4	51.4	10.2
4 <sup>d</sup>	MIL-100(Fe)	36.2	17.2	50.2	32.6
5	CuPc@MIL-101(Cr)	100	42.9	50.9	6.2
6	CuPc@MIL-100(Fe)	90.7	29.6	54.1	16.2
7 <sup>e</sup>	CuPc@MIL-101(Cr)	100	45.6	47.3	7.1
8 <sup>e</sup>	CuPc@MIL-100(Fe)	89	29.9	54.2	13.9
9 <sup>f</sup>	CuPc@MIL-101(Cr)	61.1	28.8	53.4	17.7
10 <sup>f</sup>	CuPc@MIL-100(Fe)	50.3	40.3	44.7	15

<sup>a</sup> Reaction conditions: styrene (1 mmol), catalyst (0.15 mol% based on Cu), CH<sub>3</sub>CN (2 ml), TBHP 70% (3 mmol), temperature (80 °C), time (7 h). <sup>b</sup> Other products including phenyl acetaldehyde and benzoic acid. <sup>c</sup> 0.8 mg CuPc was used. <sup>d</sup> 5 mg MOF was used. <sup>e</sup> 3rd run. <sup>f</sup> Reaction was performed at 60 °C for 4 h (identical to the reaction condition with molecular oxygen as the oxidant).

seen in the presence of TBHP as oxidant with relatively lower conversions and selectivity toward styrene oxide (Table 3, entries 3 and 4). The catalytic behavior of the bare MOFs in epoxidation reactions can be explained by the existence of coordinatively unsaturated sites (CUS) of Cr(III) in MIL-101(Cr) and the presence of Fe(III)/Fe(II) Lewis acid pairs in MIL-100(Fe), which can act as catalytic active sites [59, 60]. The reaction with the neat CuPc complex was also carried out in each oxidative system for comparison, and its results are shown in Tables 2 and 3, entry 2. After encapsulation of CuPc by assembling inside the pores of MIL-101(Cr) and MIL-100(Fe), conversion and selectivity of the resulting catalysts were conspicuously increased, especially in the reaction with O<sub>2</sub> and *iso*-butyraldehyde, in which the catalysts were more selective to styrene oxide. The reaction with CuPc@MIL-101(Cr) showed 100% conversion and 85% selectivity to styrene oxide (Table 2, entry 5), while CuPc@MIL-100(Fe) exhibited 82.8%

conversion and 76.1% selectivity to the epoxy product (Table 2, entry 6) in the O<sub>2</sub>/*iso*-butyraldehyde system. The high catalytic activity of the resulting catalysts can be justified not only by the intrinsic catalytic activity of MIL-100(Fe) and MIL-101(Cr) due to the presence of active catalytic sites as mentioned above but also by their excellent physical properties such as high surface area and pore volumes. Those textural parameters make them suitable supports for both encapsulating the CuPc complex as another active catalytic species and allowing the diffusion of guest molecules and the emergence of the products [17, 58, 61]. Although CuPc@MIL-101(Cr) and CuPc@MIL-100(Fe) exhibit high styrene conversion using TBHP as oxidant, benzaldehyde was the main product and the selectivity was lower in general than the reaction with O<sub>2</sub> and *iso*-butyraldehyde (Table 3, entries 5 and 6). With TBHP as oxidant, the reaction was also carried out under the same experimental conditions as a function of time and temperature to O<sub>2</sub>/*iso*-butyraldehyde

system, and lower conversions and selectivities were obtained (Table 3, entries 9 and 10). These results suggest that the reaction with  $O_2$ /*iso*-butyraldehyde system was more efficient than the reaction with TBHP as oxidant. Since TBHP is very toxic and not eco-friendly, therefore, molecular oxygen is an appropriate oxidant in the styrene epoxidation over the prepared catalysts. A possible reason for the lower conversion and selectivity in the case of CuPc@MIL100(Fe) could be explained by the smaller pore windows of MIL-100(Fe) (5.5 and 8.6 Å) compared to MIL-101(Cr) (16 and 19 Å), which restrict the diffusion of substrate to reach internal pores and cavities where CuPc-active sites are located [16, 20].

The evolution of the conversion of styrene as a function of reaction time employing CuPc@MIL-101(Cr) and CuPc@MIL-100(Fe) in both oxidative systems was evaluated, and results are presented in Fig. 11. As can be seen, for the  $O_2$ /*iso*-butyraldehyde system, it takes four

hours for the reactions to complete, while in the reactions with TBHP seven hours were needed for the catalysts to accomplish the best conversions.

The influence of different substituents, including electron-donating and withdrawing groups in styrene, have been further investigated in the epoxidation reaction with  $O_2$ /*iso*-butyraldehyde system under optimized reaction conditions (Table 4). The reaction with electron-withdrawing 4-chloro and 4-nitro moieties resulted in lower conversions and selectivity toward styrene oxide for both catalysts. However, in the case of electron-donating 4-methyl and 4-methoxy substituents, the epoxidation reaction in the presence of CuPc@MIL-101(Cr) as catalyst was completed in a shorter reaction time compared to the bare styrene, but when CuPc@MIL-100(Fe) was used as catalyst, although the conversions did not improve, the selectivity to the epoxy product was increased. From these results, it can be concluded that the

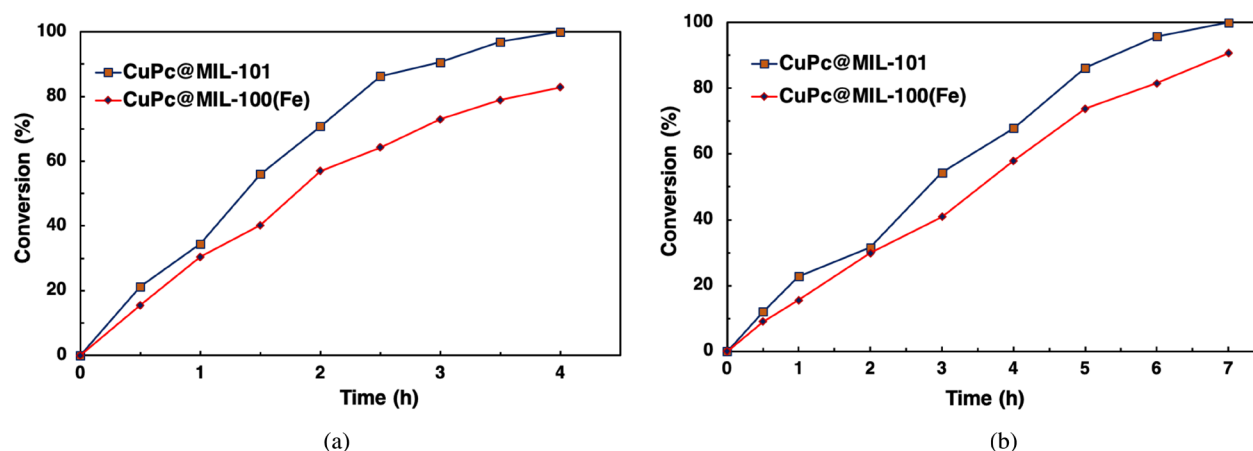


**Fig. 11.** Epoxidation of styrene catalyzed by CuPc@MIL-101(Cr) and CuPc@MIL-100(Fe) using (a)  $O_2$  as oxidant and (b) TBHP as oxidant

**Table 4.** Epoxidation of styrene derivatives with molecular oxygen<sup>a</sup>

Substrate	Catalyst	Conversion (%)	Selectivity <sup>b</sup> (%)
Styrene	CuPc@MIL-101(Cr)	100	85
	CuPc@MIL-100(Fe)	82.8	76.8
4-Chlorostyrene	CuPc@MIL-101(Cr)	86.5	64
	CuPc@MIL-100(Fe)	75.2	62.6
4-Nitrostyrene	CuPc@MIL-101(Cr)	84	71.3
	CuPc@MIL-100(Fe)	68.9	50.1
4-Methylstyrene	CuPc@MIL101(Cr) <sup>c</sup>	100	88.4
	CuPc@MIL-100(Fe)	80.7	85.2
4-Methoxystyrene	CuPc@MIL-101(Cr) <sup>d</sup>	100	85.7
	CuPc@MIL-100(Fe)	73.7	79.2

<sup>a</sup> Reaction conditions: styrene (1 mmol), catalyst (0.15 mol% based on Cu),  $CH_3CN$  (2 ml),  $O_2$  balloon (1 atm), *iso*-butyraldehyde (3 mmol), temperature (60 °C), time (4 h). <sup>b</sup> Selectivity to Styrene Oxide. <sup>c</sup> Reaction completed after 2.5 h. <sup>d</sup> Reaction completed after 3 h.



**Table 5.** Styrene epoxidation over various metallophthalocyanine-based heterogeneous catalysts

Entry	Catalyst	Oxidant	Conversion (%)	Selectivity (%)		Ref. <sup>a</sup>
				SO	B	
1	CuPcY-1(e)	TBHP	94.2	39.1	43.5	[71]
2	FePc@SiO <sub>2</sub>	Air/ <i>Iso</i> -butyraldehyde	99	74	18	[72]
3	CuPcCl <sub>16</sub> .NH <sub>2</sub> -MCM-41	TBHP	46.8	25	19	[2]
4	CuPcCl <sub>16</sub> .NH <sub>2</sub> -MCM-41	O <sub>2</sub> / <i>Iso</i> -butyraldehyde	100	74.4	20	[2]
5	Co-Pc@bio-MOF-1	TBHP	72	65	—	[43]
6	CuPcS@MC	TBHP	50	—	—	[73]
7	ZnTAPc/Gr	TBHP	73	84	—	[74]
8	CoPcTs-Zn <sub>2</sub> Al-LDH	O <sub>2</sub> / <i>Iso</i> -butyraldehyde	100	90	10	[75]
9	CuPcTs-Zn <sub>2</sub> Al-LDH	O <sub>2</sub> / <i>Iso</i> -butyraldehyde	81	86	—	[75]
10	ZnPc-MWCNTs	TBHP	96.6	86.1	10.9	[76]
11	CuPc@MIL-101(Cr)	TBHP	100	42.9	50.2	This work
12	CuPc@MIL-100(Fe)	TBHP	90.7	29.6	54.1	This work
13	CuPc@MIL-101(Cr)	O <sub>2</sub> / <i>Iso</i> -butyraldehyde	100	85	9.1	This work
14	CuPc@MIL-100(Fe)	O <sub>2</sub> / <i>Iso</i> -butyraldehyde	82.8	76.8	10.3	This work

<sup>a</sup>Experimental details and information about catalysts' structures are given in the references.

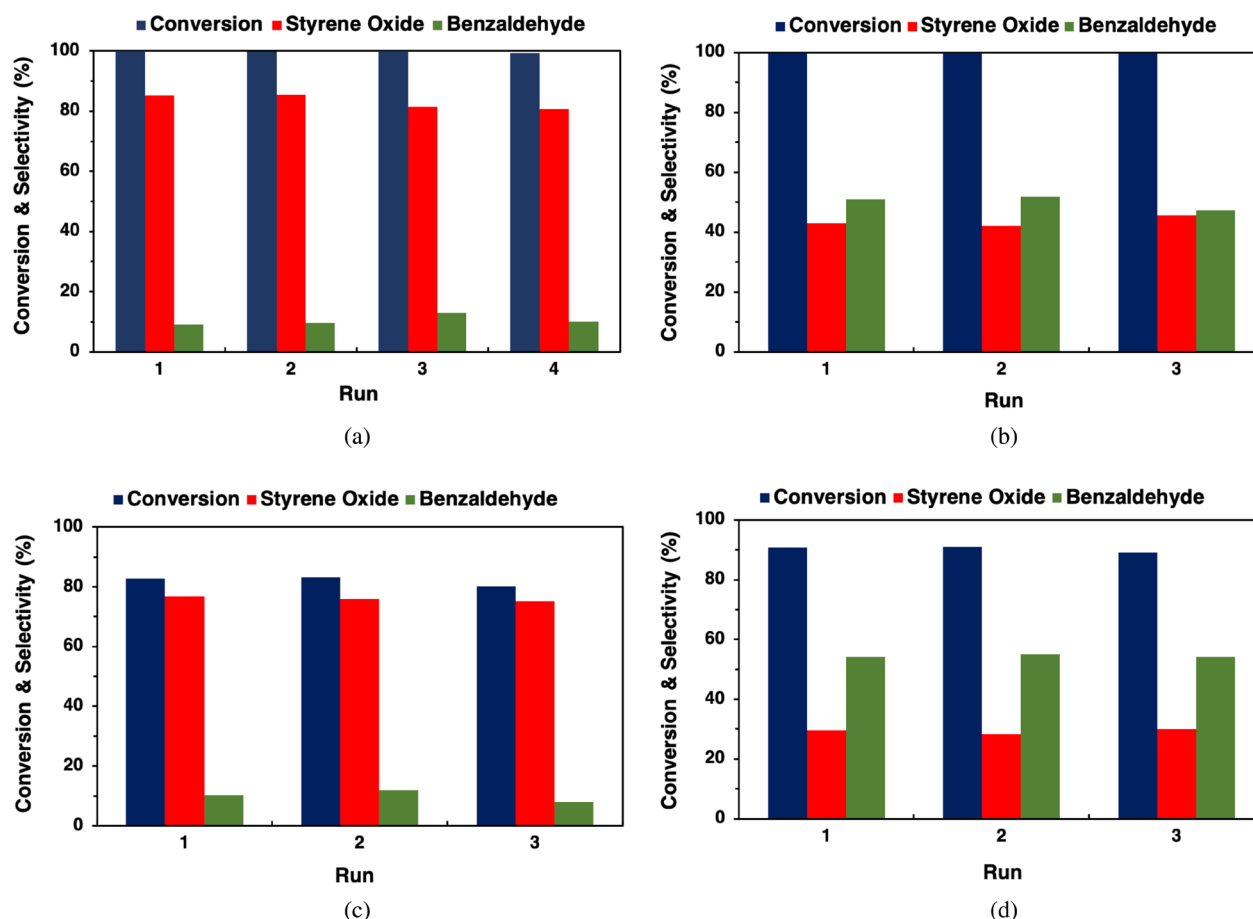
electron-donating groups on styrene prompted the double bond to be activated more readily by the enhancement of electron density, as suggested in the literature [62, 63]. Nevertheless, the steric hindrance of methyl and methoxy groups could limit the diffusion of substrates into the voids of CuPc@MIL-100(Fe) and therefore cause the conversions to be decreased compared to the styrene alone.

Table 5 summarizes the results of various MPc-based heterogeneous catalysts in the epoxidation of styrene. It is apparent that the CuPc-encapsulated MOFs used in this study demonstrate comparable results from the catalytic activity point of view, particularly in the case of the O<sub>2</sub>/*iso*-butyraldehyde oxidative system, where the catalysts were also selective toward the desirable product, styrene oxide. Although the catalysts in this study exhibited high styrene conversion when TBHP was used as the oxidant, the selectivity was poor compared to other catalysts listed in Table 4. All supports used previously to immobilize MPcs were inactive themselves, however, in this work the MOFs were catalytically active and showed a synergistic effect with CuPc as catalytically active phases in styrene epoxidation. In addition, prior functionalization of the

support or substitutions of the MPc were also necessary for most of the reported catalytic systems.

### Recyclability and heterogeneity of the catalysts

The recyclability and stability of the catalyst are essential properties of heterogeneous catalyst from economic and environmental points of view. CuPc@MIL-101(Cr) was successively recovered four times in the styrene epoxidation using O<sub>2</sub> and *iso*-butyraldehyde without a noticeable reduction in conversion, although the selectivity toward styrene oxide was slightly decreased in the fourth run (from 85% to 80.6%) (Fig. 12a). The recyclability of CuPc@MIL-101(Cr) was also tested with TBHP as oxidant, and the catalyst was recovered three times without significant loss of activity (Fig. 12b). The reusability experiment was also carried out for CuPc@MIL-100(Fe) in the presence of both O<sub>2</sub>/*iso*-butyraldehyde and TBHP as oxidants, and the results showed that this catalyst could be recovered for three cycles in both oxidative systems (Figs 12c and 12d). The PXRD patterns of the recycled catalysts indicate that the structural integrity of the catalysts was



**Fig. 12.** Recyclability of CuPc@MIL-101(Cr) in the styrene epoxidation with (a) O<sub>2</sub> as oxidant and (b) TBHP as oxidant, and CuPc@MIL-100(Fe) with (c) O<sub>2</sub> as oxidant and (d) TBHP as oxidant

**Table 6.** The amount of leached metals in the reaction solution determined by ICP-OES

Catalyst	Oxidant	Metal content (ppm)		
		Cu	Cr	Fe
CuPc@MIL-101(Cr)	O <sub>2</sub> / <i>iso</i> -butyraldehyde	0.3	0.03	—
	TBHP	0.8	0.44	—
CuPc@MIL-100(Fe)	O <sub>2</sub> / <i>iso</i> -butyraldehyde	0.75	—	1.13
	TBHP	≈1	—	1.92

preserved after consecutive runs (Figs S1–S2, Supporting information). The FT-IR spectra of the catalysts after final runs demonstrated that the characteristic bands of the samples were also maintained (Figs S3–S4). The UV-DR spectra of the spent catalysts exhibited no significant shifts of absorption peaks, although in the case of recovered CuPc@MIL-101(Cr) in the reaction with TBHP as oxidant and recovered CuPc@MIL-100(Fe) in both oxidative systems, the broadening of absorption bands was observed which is attributed to aggregation of the CuPc complex (Figs S5–S6) [64]. The TEM images

observed after the catalytic reactions with both TBHP and O<sub>2</sub>/*iso*-butyraldehyde displayed no significant changes in the catalysts' shapes and morphology (Fig. S7).

The investigation of heterogeneity of the catalysts was conducted by hot filtration tests and the reaction solution was analyzed by ICP-OES after removing the catalysts to examine possible leaching of transition metals. Table 6 shows the amount of metals leached into the reaction media. As can be observed, the amounts of leached metals are below or around 1 ppm in the reaction with O<sub>2</sub> and TBHP as oxidants, respectively. It is worth mentioning

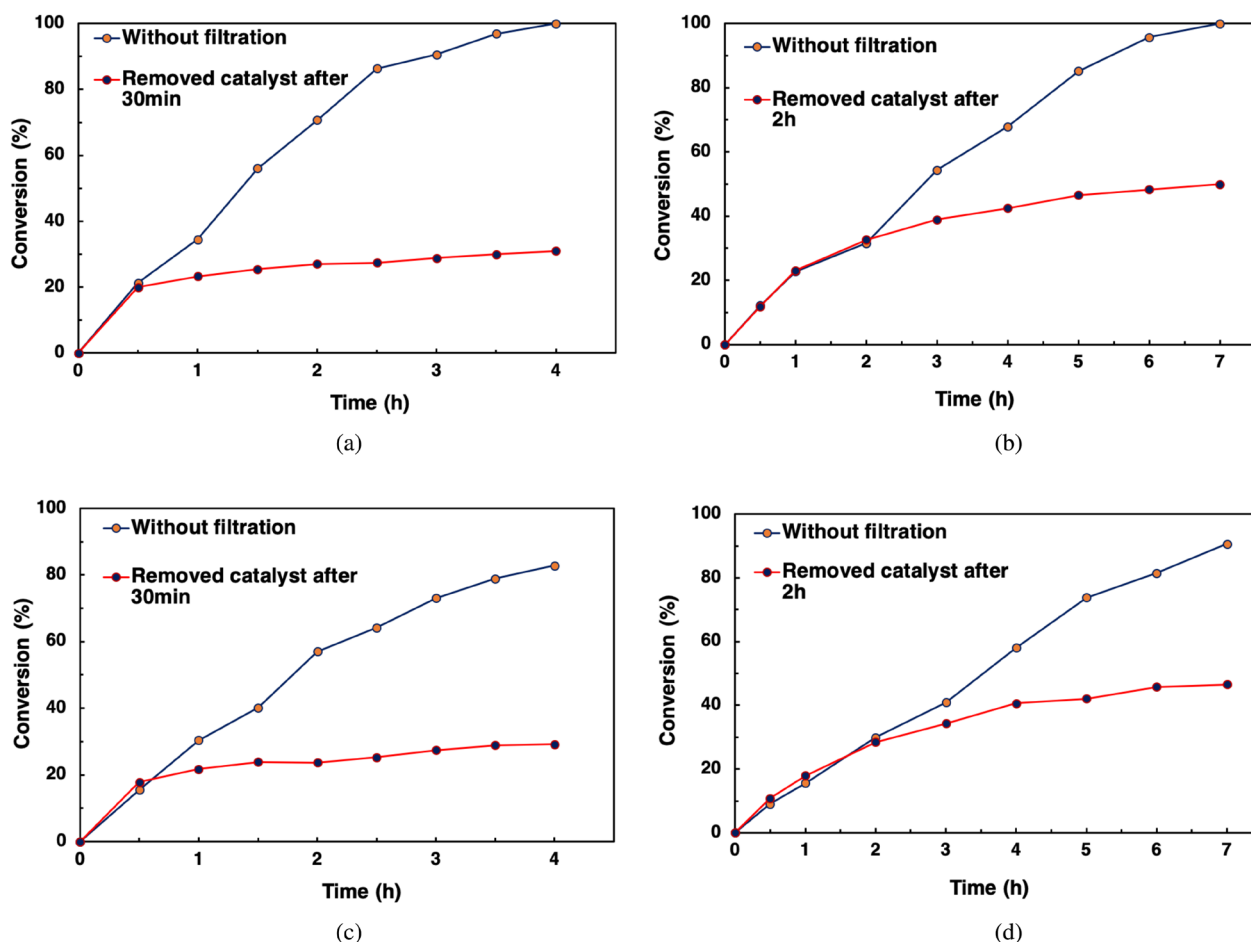


Fig. 13. Hot filtration tests of (a) CuPc@MIL-101(Cr) with  $O_2$  as oxidant, (b) CuPc@MIL-101(Cr) with TBHP as oxidant, (c) CuPc@MIL-100(Fe) with  $O_2$  as oxidant and (d) CuPc@MIL-100(Fe) with TBHP as the oxidant in the styrene epoxidation

that such amounts of leached metal are acceptable in the production of fine chemicals [65]. Hot filtration tests were also carried out in both oxidative systems, and the results are shown in Fig. 13. The catalysts were filtered off after 30 min in the reaction with  $O_2$ /iso-butylaldehyde and after two hours in the case where TBHP was the oxidant. After removing the catalysts, the progress of each reaction was dramatically decreased; this confirms the heterogeneous route of the reaction.

## EXPERIMENTAL

### Materials

All compounds were not purified and used as purchased.  $Cr(NO_3)_3 \cdot 9H_2O$ ,  $CuCl_2$ ,  $Fe(NO_3)_3 \cdot 9H_2O$ , *tert*-butyl hydroperoxide (TBHP) 70% aqueous solution, terephthalic acid (TPA) and styrene were acquired from Merck. Trimesic acid ( $H_3BTC$ ), *iso*-butylaldehyde, choline chloride, and urea were procured from Sigma-Aldrich. All the solvents were of analytical grade and obtained from Daejung Chemicals. Deep eutectic solvent

(DES) was prepared by a previously reported procedure [66]. Copper phthalocyanine (CuPc) was also synthesized by a recently described method [45] from a mixture of copper(II) chloride salt and phthalonitrile in the presence of DES and employed as the homogeneous catalyst for comparison.

### Characterizations

The powder X-ray diffraction (PXRD) patterns were collected on an STOE diffractometer using  $K\alpha$  radiation ( $\lambda = 1.5418 \text{ \AA}$ ). The FT-IR spectra were measured on a Bomem MB-Series FT-IR spectrometer using the KBr pellet method. The Cu contents in the compounds were obtained using an inductively coupled plasma-optical emission spectrometer (ICP-OES) with a Varian Vista-PRO instrument. The UV-vis spectra of the materials were determined with a Shimadzu UV-2100 spectrophotometer. The diffuse reflectance UV spectra were acquired on a Shimadzu UV-2550 spectrophotometer. The scanning electron microscopy images were obtained with a Hitachi SU3500 scanning electron microscope. TEM images were taken by a Philips

CM30 scanning transmission electron microscope. Nitrogen adsorption-desorption isotherms were recorded at  $-196^{\circ}\text{C}$  with a BELSORP-Mini II high precision surface area and pore size analyzer. The samples were degassed at  $150^{\circ}\text{C}$  for 12 h prior measurements. The specific surface area was calculated by the Brunner–Emmet–Teller (BET) equation.

### Preparation of MIL-101(Cr)

MIL-101(Cr) was synthesized based on a reported hydrofluoric acid (HF)-free procedure [67]. Briefly, a mixture of  $\text{Cr}(\text{NO}_3)_3 \cdot 9\text{H}_2\text{O}$  (5 mmol), TPA (5 mmol), and deionized (DI) water (20 mL) was dispersed by short sonication. Then the suspension was placed in a hydrothermal autoclave reactor and kept for 18 h at  $218^{\circ}\text{C}$ . The green solid was collected by centrifugation, washed with distilled water and acetone, and soaked in 20 mL DMF at  $70^{\circ}\text{C}$  for 12 h to eliminate any unreacted linker trapped within the pores. The resulting material was separated by centrifuge, washed with methanol and acetone, and dried under vacuum at  $150^{\circ}\text{C}$  for 12 h before further use.

### Preparation of MIL-100(Fe)

MIL-100(Fe) was prepared in an HF-free solution, according to the procedure described in the literature [68]. Firstly,  $\text{Fe}(\text{NO}_3)_3 \cdot 9\text{H}_2\text{O}$  (18 mmol) was added to 18 mL DI water and stirred until fully dissolved. Then,  $\text{H}_3\text{BTC}$  (12 mmol) was added, and the mixture was stirred for 1 h. The obtained mixture was transferred into an 80 mL Teflon-lined stainless steel autoclave and kept at  $160^{\circ}\text{C}$  for 15 h. After cooling down the autoclave to room temperature, the orange solid was collected by centrifugation, washed with 180 mL water at  $70^{\circ}\text{C}$  for 3 h and then 180 mL ethanol at  $65^{\circ}\text{C}$  for another 3 h. The obtained powder was recovered by centrifuge, dried at  $80^{\circ}\text{C}$  overnight and then at  $150^{\circ}\text{C}$  under vacuum for 12 h before use.

### Preparation of $\text{Cu}^{2+}$ @MIL-101(Cr) and $\text{Cu}^{2+}$ @MIL-100(Fe)

The loading of  $\text{Cu}^{2+}$  inside the pores of MIL-100(Fe) and MIL-101(Cr) was done *via* a double-solvent approach [69, 70]. Typically, 200 mg of activated MIL-101(Cr) was suspended in 40 mL dry *n*-hexane as a hydrophobic solvent and sonicated for 25 min until homogeneous suspension achieved. 0.123 mL of 1 M aqueous solution of  $\text{CuCl}_2$  as a hydrophilic solvent was added dropwise under constant intense stirring. After continuous stirring for 3 h, the obtained powder was recovered and dried in vacuum at  $150^{\circ}\text{C}$  for 12 h. In the case of MIL-100(Fe), the same procedure was employed except the amount of added  $\text{CuCl}_2$  solution added was 0.100 mL, since the total pore volume of the MIL-100(Fe) was smaller than MIL-101(Cr) as revealed by nitrogen adsorption measurements.

### Synthesis of $\text{CuPc}$ @MIL-101(Cr) and $\text{CuPc}$ @MIL-100(Fe)

To 200 mg of dried  $\text{Cu}^{2+}$ @MIL-101(Cr), 2 mL of ethanol was added and briefly sonicated. Then, phthalonitrile (0.492 mmol) was added to the suspension and stirred for 1 h. After that, ethanol was removed under reduced pressure, and 2 mL of DES was added to the resulting solid. Afterward, the mixture was heated to  $150^{\circ}\text{C}$  for 30 min to obtain  $\text{CuPc}$ @MIL-101(Cr) as revealed by the deep blue color of the as-prepared catalyst.  $\text{CuPc}$ @MIL-100(Fe) was prepared by the same procedure except that 0.400 mmol phthalonitrile in ethanol was added to the  $\text{Cu}^{2+}$ @MIL-100(Fe) suspension, and the resulting mixture was stirred for 3 h. The synthesized catalysts were dried and activated under vacuum at  $150^{\circ}\text{C}$  overnight before the catalytic run.

### Catalytic test

The catalytic styrene epoxidation was carried out in a 10 mL PTFE screw cap glass vial with septa. In a typical experiment, styrene (1 mmol), catalyst (0.15 mol% based on Cu) and *iso*-butyraldehyde (3 mmol) were added to acetonitrile (2 mL) as the solvent. Subsequently, an oxygen balloon was placed at the top of the glass vial, and the reaction mixture was heated to  $60^{\circ}\text{C}$  for 4 h. After the reaction was completed, the catalyst was recovered by centrifuge, washed thoroughly with acetonitrile and dried at  $150^{\circ}\text{C}$  under reduced pressure for 12 h before the next run. The products were examined with a gas chromatograph (Agilent 7890A) equipped with a BP-5 capillary column and an FID detector. The reaction with TBHP 70% was carried out, except 3 mmol of TBHP was used instead of the  $\text{O}_2$  balloon and reductant.

## CONCLUSIONS

In summary, copper phthalocyanine ( $\text{CuPc}$ ) complex was synthesized and encapsulated inside the pores of MIL-100(Fe) and MIL-101(Cr) with a more convenient approach than the reported strategies utilizing deep eutectic solvent (DES) in shorter reaction time and lower temperature. The prepared materials were employed as heterogeneous catalysts in the epoxidation of styrene with  $\text{O}_2$  and aqueous TBHP as oxidants in two optimized reaction conditions. The catalysts demonstrated excellent catalytic activity, especially with molecular oxygen as a green oxidant with high conversion (100% with  $\text{CuPc}$ @MIL-101(Cr) vs. 82.8% with  $\text{CuPc}$ @MIL-100(Fe)) and selectivity toward styrene oxide (85% with  $\text{CuPc}$ @MIL-101(Cr) vs. 76.8% with  $\text{CuPc}$ @MIL-100(Fe)) as the desired product. Moreover, the catalysts can be recovered and reused several times without considerable drops in activity, and they also are stable after reuse as demonstrated by PXRD, FT-IR, and UV-DRS techniques. Finally, the leaching experiments, combined



with ICP-OES results, illustrated that the catalysts are genuinely heterogeneous.

## Acknowledgments

The authors thank the Vice-President's Office for Research Affairs of the Shahid Beheshti University for supporting this work.

## Supporting information

Characterizations of spent catalysts (Figs S1–S7) are given in the supplementary material, which is available free of charge via the internet at <http://www.worldscinet.com/jpp/jpp.shtml>.

## REFERENCES

- Choudhary VR, Jha R and Jana P. *Green Chem.* 2006; **8**: 689–690.
- Karandikar P, Agashe M, Vijayamohanan K and Chandwadkar AJ. *Appl. Catal. A* 2004; **257**: 133–143.
- Corma A and García H. *Chem. Rev.* 2002; **102**: 3837–3892.
- Judge JM. *J. Polym. Sci., Part B: Polym. Lett.* 1972; **10**: 230–231.
- Punniyamurthy T, Velusamy S and Iqbal J. *Chem. Rev.* 2005; **105**: 2329–2364.
- Tyagi B, Sharma U and Jasra RV. *Appl. Catal. A* 2011; **408**: 171–177.
- Zhang A, Li L, Li J, Zhang Y and Gao S. *Catal. Commun.* 2011; **12**: 1183–1187.
- Wu C De. In *Selective Nanocatalysts and Nanoscience: Concepts for Heterogeneous and Homogeneous Catalysis*. Vol 110. Zecchina A, Bordiga S and Groppo E. (Eds). Wiley-VCH: Weinheim, Germany, 2011, pp. 271–298.
- Dhakshinamoorthy A, Alvaro M and Garcia H. *Chem. Commun.* 2012; **48**: 11275–11288.
- Dhakshinamoorthy A, Alvaro M and Garcia H. *Catal. Sci. Technol.* 2011; **1**: 856–867.
- Furukawa H, Ko N, Go YB, Aratani N, Choi SB, Choi E, Yazaydin AO, Snurr RQ, O'Keeffe M, Kim J and Yaghi OM. *Science* (80-). 2010; **329**: 424–428.
- Schneemann A, Bon V, Schwedler I, Senkovska I, Kaskel S and Fischer RA. *Chem. Soc. Rev.* 2014; **43**: 6062–6096.
- Eddaoudi M, Kim J, Rosi N, Vodak D, Wachter J, O'Keeffe M and Yaghi OM. *Science* (80-). 2002; **295**: 469–472.
- Wu F, Qiu LG, Ke F and Jiang X. *Inorg. Chem. Commun.* 2013; **32**: 5–8.
- Shaabani A, Mohammadian R, Farhid H, Karimi Alavijeh M and Amini MM. *Catal. Lett.* 2019; **149**: 1237–1249.
- Horcajada P, Surblé S, Serre C, Hong DY, Seo YK, Chang JS, Grenèche JM, Margiolaki I and Férey G. *Chem. Commun.* 2007; **0**: 2820–2822.
- Hong DY, Hwang YK, Serre C, Férey G and Chang JS. *Adv. Funct. Mater.* 2009; **19**: 1537–1552.
- Hwang YK, Hong DY, Chang JS, Jung SH, Seo YK, Kim J, Vimont A, Daturi M, Serre C and Férey G. *Angew. Chem., Int. Ed.* 2008; **47**: 4144–4148.
- Férey G, Serre C, Mellot-Draznieks C, Millange F, Surblé S, Dutour J and Margiolaki I. *Angew. Chem., Int. Ed.* 2004; **43**: 6296–6301.
- Férey C, Mellot-Draznieks C, Serre C, Millange F, Dutour J, Surblé S and Margiolaki I. *Science* (80-). 2005; **309**: 2040–2042.
- Boroujeni MB, Hashemzadeh A, Faroughi M-T, Shaabani A and Amini MM. *RSC Adv.* 2016; **6**: 100195–100202.
- Shaabani A, Sepahvand H, Amini MM, Hashemzadeh A, Borjian Boroujeni M and Badali E. *Tetrahedron* 2018; **74**: 1832–1837.
- Li H, Shi W, Zhao K, Li H, Bing Y and Cheng P. *Inorg. Chem.* 2012; **51**: 9200–9207.
- Dhakshinamoorthy A, Alvaro M, Concepcion P and Garcia H. *Catal. Commun.* 2011; **12**: 1018–1021.
- Tonigold M, Lu Y, Mavrandonakis A, Puls A, Staudt R, Möllmer J, Sauer J and Volkmer D. *Chem. — Eur. J.* 2011; **17**: 8671–8695.
- Maksimchuk NV, Kovalenko KA, Arzumanov SS, Chesalov YA, Melgunov MS, Stepanov AG, Fedin VP and Kholdeeva OA. *Inorg. Chem.* 2010; **49**: 2920–2930.
- Abednatanzi S, Abbasi A and Masteri-Farahani M. *Catal. Commun.* 2017; **96**: 6–10.
- Shah WA, Noureen L, Nadeem MA and Kögerler P. *J. Solid State Chem.* 2018; **268**: 75–82.
- Ke F, Zhu J, Qiu LG and Jiang X. *Chem. Commun.* 2013; **49**: 1267–1269.
- Brammer L, Xiao J, Grigoropoulos A, Weller AS, Katsoulidis AP, Rosseinsky MJ, Haynes A, Davies RP and McKay AI. *Angew. Chem., Int. Ed.* 2018; **57**: 4532–4537.
- Zhang F, Jin Y, Fu Y, Zhong Y, Zhu W, Ibrahim AA and El-Shall MS. *J. Mater. Chem. A* 2015; **3**: 17008–17015.
- Hashemzadeh A, Amini MM, Tayebbe R, Sadeghian A, Durndell LJ, Isaacs MA, Osatiashtiani A, Parlett CMA and Lee AF. *Mol. Catal.* 2017; **440**: 96–106.
- Hauser SA, Cokoja M and Kühn FE. *Catal. Sci. Technol.* 2013; **3**: 552–561.
- Gupta KC and Sutar AK. *Coord. Chem. Rev.* 2008; **252**: 1420–1450.
- Herrmann WA and Cornils B. *Angew. Chem., Int. Ed. Engl.* 1997; **36**: 1048–1067.
- Dai LX. *Angew. Chem., Int. Ed.* 2004; **43**: 5726–5729.
- Collis AEC and Horváth IT. *Catal. Sci. Technol.* 2011; **1**: 912–919.
- Sorokin AB. *Chem. Rev.* 2013; **113**: 8152–8191.

39. Pirouzmmand M, Amini MM and Safari N. *J. Colloid Interface Sci.* 2008; **319**: 199–205.
40. Shaabani A, Mohammadian R, Hashemzadeh A, Afshari R and Amini MM. *New J. Chem.* 2018; **42**: 4167–4174.
41. Zalomaeva OV, Kovalenko KA, Chesalov YA, Mel'Gunov MS, Zaikovskii VI, Kaichev VV, Sorokin AB, Kholdeeva OA and Fedin VP. *Dalton Trans.* 2011; **40**: 1441–1444.
42. Kockrick E, Lescouet T, Kudrik EV, Sorokin AB and Farrusseng D. *Chem. Commun.* 2011; **47**: 1562–1564.
43. Li B, Zhang Y, Ma D, Ma T, Shi Z and Ma S. *J. Am. Chem. Soc.* 2014; **136**: 1202–1205.
44. Boroujeni MB, Hashemzadeh A, Shaabani A and Amini MM. *Appl. Organomet. Chem.* 2017; **31**: e3715.
45. Shaabani A, Hooshmand SE, Afshari R, Shaabani S, Ghasemi V, Atharnezhad M and Akbari M. *J. Solid State Chem.* 2018; **258**: 536–542.
46. Ferreira RB, Scheetz PM and Formiga ALB. *RSC Adv.* 2013; **3**: 10181–10184.
47. Liu Q, Ning L, Zheng S, Tao M, Shi Y and He Y. *Sci. Rep.* 2013; **3**: 2916.
48. Lv H, Zhao H, Cao T, Qian L, Wang Y and Zhao G. *J. Mol. Catal. A* 2015; **400**: 81–89.
49. Huang S, Yang KL, Liu XF, Pan H, Zhang H and Yang S. *RSC Adv.* 2017; **7**: 5621–5627.
50. Çaylak Delibaş N, Gündüz B, Bilgiçli AT, Pişkin H, Günsel A and Yarasir MN. *New J. Chem.* 2018; **42**: 6013–6022.
51. Kholghi Eshkalak S, Khatibzadeh M, Kowsari E, Chinnappan A and Ramakrishna S. *Dyes Pigm.* 2018; **154**: 296–302.
52. Eastwood D, Edwards L, Gouterman M and Steinfield J. *J. Mol. Spectrosc.* 1966; **20**: 381–390.
53. Mack J and Stillman MJ. *Coord. Chem. Rev.* 2001; **219–221**: 993–1032.
54. Seelan S, Agashe MS, Srinivas D and Sivasanker S. *J. Mol. Catal. A* 2001; **168**: 61–68.
55. Tanamura Y, Uchida T, Teramae N, Kikuchi M, Kusaba K and Onodera Y. *Nano Lett.* 2001; **1**: 387–390.
56. Hamza A and Srinivas D. *Catal. Lett.* 2009; **128**: 434–442.
57. Thommes M, Kaneko K, Neimark AV, Olivier JP, Rodriguez-Reinoso F, Rouquerol J and Sing KSW. *Pure Appl. Chem.* 2015; **87**: 1051–1069.
58. Wan H, Chen C, Wu Z, Que Y, Feng Y, Wang W, Wang L, Guan G and Liu X. *ChemCatChem* 2015; **7**: 441–449.
59. Sun J, Yu G, Huo Q, Kan Q and Guan J. *RSC Adv.* 2014; **4**: 38048–38054.
60. Dhakshinamoorthy A, Alvaro M, Horcajada P, Gibson E, Vishnuvarthan M, Vimont A, Grenèche JM, Serre C, Daturi M and Garcia H. *ACS Catal.* 2012; **2**: 2060–2065.
61. Henschel A, Gedrich K, Kraehnert R and Kaskel S. *Chem. Commun.* 2008; **0**: 4192–4194.
62. Tang Y, Gao H, Yang M, Wang G, Li J, Zhang H and Tao Z. *New J. Chem.* 2016; **40**: 8543–8548.
63. Bian G, Jiang P, Zhao H, Jiang K, Hu L, Dong Y and Zhang W. *ChemistrySelect* 2016; **1**: 1384–1392.
64. Touka N, Benelmadjat H, Boudine B, Halimi O and Sebais M. *J. Assoc. Arab Univ. Basic Appl. Sci.* 2013; **13**: 52–56.
65. Sheldon RA, Wallau M, Arends IWCE and Schuchardt U. *Acc. Chem. Res.* 1998; **31**: 485–493.
66. Abbott AP, Capper G, Davies DL, Rasheed RK and Tambyrajah V. *Chem. Commun.* 2003; **0**: 70–71.
67. Bromberg L, Diao Y, Wu H, Speakman SA and Hutton TA. *Chem. Mater.* 2012; **24**: 1664–1675.
68. Seo YK, Yoon JW, Lee JS, Lee UH, Hwang YK, Jun CH, Horcajada P, Serre C and Chang JS. *Microporous Mesoporous Mater.* 2012; **157**: 137–145.
69. Aijaz A, Karkamkar A, Choi YJ, Tsumori N, Rönnebro E, Autrey T, Shioyama H and Xu Q. *J. Am. Chem. Soc.* 2012; **134**: 13926–13929.
70. Yadav M and Xu Q. *Chem. Commun.* 2013; **49**: 3327–3329.
71. Seelan S, Sinha AK, Srinivas D and Sivasanker S. *J. Mol. Catal. A* 2000; **157**: 163–171.
72. Mangematin S and Sorokin AB. *J. Porphyrins Phthalocyanines* 2001; **5**: 674–680.
73. Manna J, Amali AJ and Rana RK. *Chem. — Eur. J.* 2014; **20**: 8453–8457.
74. Ju L, Mei J, Li Z and Xu S. *Fullerenes, Nanotubes, Carbon Nanostruct.* 2017; **25**: 423–428.
75. Zhou W, Zhou J, Chen Y, Cui A, Sun F, He M, Xu Z and Chen Q. *Appl. Catal. A* 2017; **542**: 191–200.
76. Li Q, Sun Z, Zhou M, Liang Q, Li Z and Xu S. *J. Mater. Sci.: Mater. Electron.* 2019; **30**: 6277–6286.